Molecular Cell
Article

Expression Noise and Acetylation Profiles Distinguish HDAC Functions

Leehee Weinberger,[1,3] Yoav Voichek,[1,3] Itay Tirosh,[1] Gil Hornung,[1] Ido Amit,[2] and Naama Barkai[1,*]
[1]Department of Molecular Genetics
[2]Department of Immunology
Weizmann Institute of Science, Rehovot, Israel
[3]These authors contributed equally to this work
*Correspondence: naama.barkai@weizmann.ac.il
DOI 10.1016/j.molcel.2012.05.008

SUMMARY

Gene expression shows a significant variation (noise) between genetically identical cells. Noise depends on the gene expression process regulated by the chromatin environment. We screened for chromatin factors that modulate noise in *S. cerevisiae* and analyzed the results using a theoretical model that infers regulatory mechanisms from the noise versus mean relationship. Distinct activities of the Rpd3(L) and Set3 histone deacetylase complexes were predicted. Both HDACs repressed expression. Yet, Rpd3(L)C decreased the frequency of transcriptional bursts, while Set3C decreased the burst size, as did H2B monoubiquitination (ubH2B). We mapped the acetylation of H3 lysine 9 (H3K9ac) upon deletion of multiple subunits of Set3C and Rpd3(L)C and of ubH2B effectors. ubH2B and Set3C appear to function in the same pathway to reduce the probability that an elongating PolII produces a functional transcript (PolII processivity), while Rpd3(L)C likely represses gene expression at a step preceding elongation.

INTRODUCTION

Cells that are genetically identical may still behave differently under identical conditions (Barkai and Shilo, 2007; Raser and O'Shea, 2005). This nongenetic variability is largely due to noise in gene expression (Bar-Even et al., 2006; Elowitz et al., 2002; Ozbudak et al., 2002). Noise varies between genes, and to a first approximation, it decreases with mean abundance. Yet, many genes deviate from this general trend (Bar-Even et al., 2006; Newman et al., 2006). For example, the low noise of essential genes and the high noise of stress-related genes are not explained by differences in mean abundance, but instead may depend on differences in the underlying gene expression mechanisms.

The prevailing model of gene expression noise assumes that proteins are made in "bursts": short time intervals in which proteins are produced, interspaced by periods of negligible production (Blake et al., 2003; Cai et al., 2006; Tan and van Oudenaarden, 2010; Zenklusen et al., 2008). The main stochastic event is burst initiation. Noise is amplified by the burst size (number of proteins made per burst), such that for a given level of mean expression, variability increases in proportion to burst size (Paulsson, 2004; Tan and van Oudenaarden, 2010). Burst frequency and burst size can be estimated from the distribution of expression levels: Let μ and η^2 denote the respective mean and coefficient of variation (noise) of the expression distribution. The predicted burst size and burst frequency are estimated by $\eta^{2*}\mu$ and η^{-2}, respectively. Burst size is therefore the normalized variance, accounting for the inherent link between the noise and mean expression (Friedman et al., 2006; Raj et al., 2006; Tan and van Oudenaarden, 2010).

A key implication of this model is that gene expression can be regulated in two principally different ways. Regulation of burst frequency will coordinately modify mean expression and noise. By contrast, regulation of burst size will change mean expression, but will not alter the coefficient of variation. Therefore, when studying the effect of a regulator of interest on gene expression, it may be beneficial to examine both mean expression and noise. Mean expression will distinguish between activators and repressors while noise may distinguish between regulators of burst frequency versus regulators of burst size.

Identifying regulators of burst size is of a particular interest, as it provides insight to noise control. We used the model organism *S. cerevisiae* to search for regulators of burst size among chromatin-associated factors. Chromatin affects gene expression directly, by restricting DNA accessibility, and indirectly, by recruiting other factors (Henikoff and Shilatifard, 2011). Previous reports implicated chromatin in noise regulation. First, genes of high noise are associated with promoters that lack the typical nucleosome-free region (NFR). These promoters, termed Occupied Proximal Nucleosome (OPN), show increased sensitivity to regulation by multiple chromatin factors (Blake et al., 2006; Cairns, 2009; Field et al., 2009; Tirosh and Barkai, 2008). Furthermore, individual deletions of three chromatin factors, the acetyl-transferase *GCN5* and the chromatin remodelers *SNF6* and *ARP8*, increased expression noise driven by the inducible PHO5 promoter (Raser and O'Shea, 2004). Recent systematic assays for noise regulators using a specific reporter also pointed to chromatin-associated factors (Rinott et al., 2011).

Motivated by this data, we screened 137 nonessential chromatin factors for modifiers of the normalized noise (the

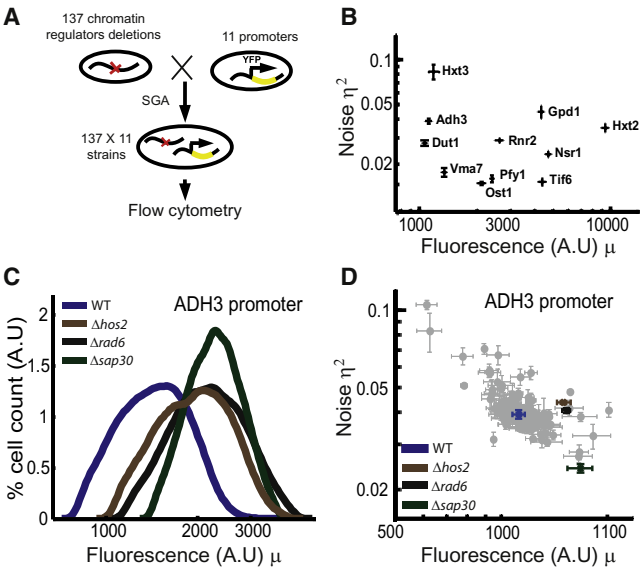

Figure 1. Screen for Chromatin Regulators that Change Gene Expression Noise

(A) Screen design: 137 strains deleted of individual chromatin-associated factors were obtained from the yeast deletion library. Each mutant was combined with 11 strains carrying YFP under a specific reporter promoter using the SGA method. All together, 137*11 strains were analyzed. For each strain, the single-cell distribution of fluorescence levels was measured using flow cytometry.

(B) Noise versus mean relationship for the reporters used in the screen: the distribution of single-cell YFP expression levels driven by the reporter promoters was measured in a wild-type background. Error bars represent standard error over multiple independent measurements. We define the noise η^2 as the coefficient of variation.

(C) Distribution of expression levels: histograms of single-cell YFP expression levels driven by ADH3 promoter for the strains indicated. Cells were gated by the Forward-scattering and Side-scattering measures, to ensure a similar cell-cycle phase and cell size.

(D) Noise versus mean relationship for the ADH3 promoter in all mutant backgrounds: each point represents the noise and mean of YFP expression driven by the ADH3 promoter in one of the 137 mutant backgrounds. Error bars represent standard error over three independent measurements. See also Figure S1 and Table S1.

predicted burst size). We initially hypothesized that burst size is regulated primarily at the level of burst duration, likely depending on the promoter or 5′ end of genes. Surprisingly, the modification that had the strongest predicted (repressive) effect on burst size was H2B monoubiquitination (ubH2B), which is generally associated with transcription elongation (Fleming et al., 2008; Pavri et al., 2006; Shilatifard, 2006) and is found primarily within the coding region (Schulze et al., 2009). The second process identified was Set3C-dependent deacetylation. Similar to ubH2B, Set3C was also associated with transcription elongation. Further, at least in certain cases, its recruitment depends on H3K4 dimethylation, which is promoted by ubH2B (Kim and Buratowski, 2009; Wang et al., 2002).

PolII processivity is an elongation-related process affecting burst size. This measure defines the probability that an elongating PolII will produce a functional transcript, rather than terminate prematurely (Mason and Struhl, 2005). Theoretically, when burst events are well separated in time, burst size increases linearly with PolII processivity. Notably, since burst size is the total number of proteins made per burst, other aspects affecting elongation (e.g., elongation velocity) will modulate burst size only through their effect on PolII processivity. We therefore hypothesized that both ubH2B and Set3C-dependent deacetylation repress PolII processivity and examined this hypothesis using several high-throughput data sets.

Set3C is one of multiple histone deacetylation complexes (HDACs) expressed in *S. cerevisiae*. HDAC complexes are extensively studied, yet their individual functions are only partially understood (Kurdistani and Grunstein, 2003). The predicted role of Set3C in decreasing burst size was of particular interest to us, as it differed from the predicted function of other HDACs. The well-studied Rpd3(L) complex, for example, repressed the predicted burst frequency and not the burst size. Furthermore, while Rpd3(L)C is known to act as a repressor of gene expression (Kurdistani and Grunstein, 2003; Robyr et al., 2002), Set3C is required for the rapid induction of the Gal1 gene (Kim and Buratowski, 2009; Wang et al., 2002). Our data, on the other hand, suggest that Set3C, like Rpd3(L)C, acts primarily as a repressor of gene expression, albeit through different means. We therefore explored further the distinct activities of these two complexes.

HDAC activities can be distinguished by their effect on the genome-wide histone acetylation. Such mapping revealed, for example, a "division of labor" between HDACs acting on different gene promoters (Robyr et al., 2002; Wang et al., 2002). Existing data reporting acetylation profiles in Rpd3(L)C and Set3C mutant background, however, mapped acetylation at promoter only, and are of a low spatial resolution. To examine the role of Set3C in transcription elongation and PolII processivity, and to test whether ubH2B and Set3C function in the same pathway, we wished to examine acetylation profiles in mutants affecting histone acetylation and ubH2B. We therefore generated a high-resolution map of H3K9 acetylation in five mutants deleted of Set3C and Rpd3(L)C components and in four mutants deleted of ubH2B effectors. These data were analyzed in combination with existing functional genomic data sets. Based on this, we now provide evidence that ubH2B and Set3-dependent deacetylation function in the same pathway to reduce PolII processivity, while Rpd3(L)C's key role in gene repression precedes elongation.

RESULTS

Screening for Chromatin Regulators of Gene Expression Noise

We selected 137 chromatin factors and tested how their individual deletions modulate the expression (mean and variance) of a fluorescence reporter driven by one of 11 representative promoters (Figure 1A). Our screen covered most of the nonessential chromatin modifiers, including regulators of histone acetylation, methylation, phosphorylation or ubiquitination, chromatin remodelers, histone variant, exchange factors, elements of the general transcription machinery, and chromatin silencing genes (Table S1). The 11 promoters used as reporters spanned a range of intermediate expression levels that are high

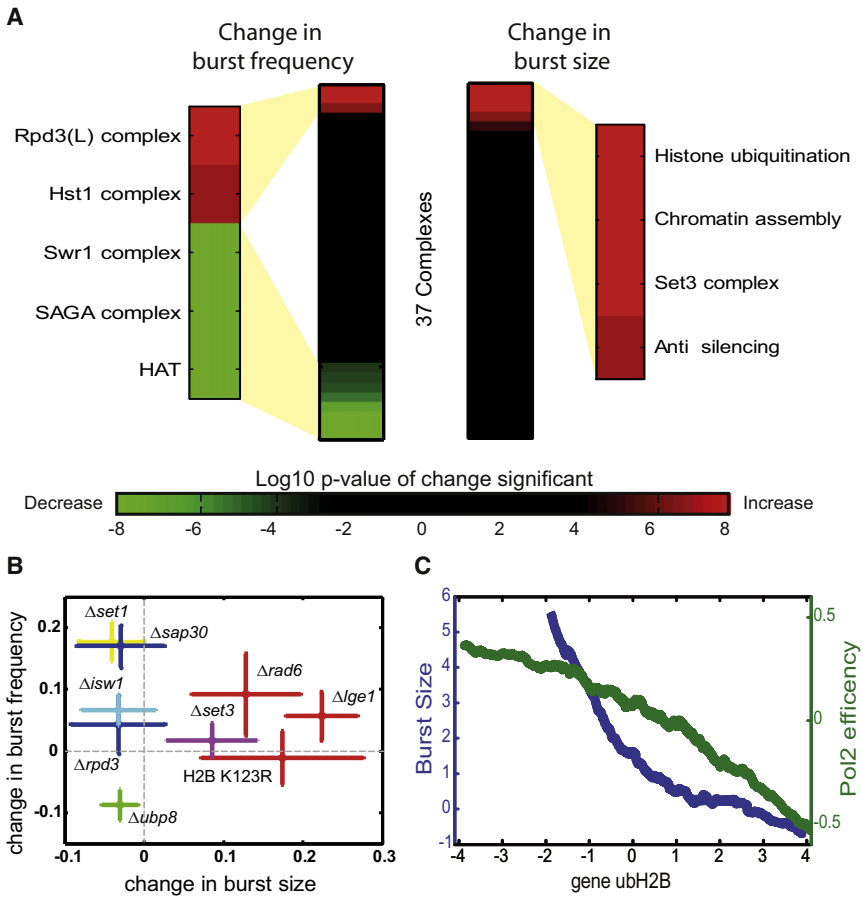

Figure 2. Effectors of Burst Size and Burst Frequency

(A) Complexes affecting burst size or burst frequency: the 137 chromatin regulators assayed in the screen were sorted into 37 complexes based on their function and interactions (Table S1). Fisher's method was used to calculate the effect of each complex on burst size and frequency of all 11 promoters, based on the expression distribution of each of the strains corresponding to its individual constituents. The complexes were sorted and ranked by the strength and the direction of their effect. The color bar corresponds to significance of the changes observed (log10 of p value).

(B) Deletion affecting burst size or burst frequency: the effect of specific deletions on burst size and frequency was verified using additional 200 GFP-fusion reporters. The median change in burst frequency ([mutant − WT] ÷ WT) is plotted as a function of the median change in burst size. The colors correspond to the different complexes/functions: Rpd3(L) histone deacetylation complex (Δ*sap30*, Δ*rpd3*), blue; Set3 histone deacetylation complex (Δ*set3*), magenta; histone methylation (Δ*set1*), yellow; nucleosome remodeling (Δ*isw1*), cyan; histone deubiquitination (Δ*ubp8*), green; and histone ubiquitination (Δ*rad6*, Δ*lge1*, *h2b-K123R* [histone mutant unable to go through ubiquitination]), red. Error bars represent standard errors.

(C) Genomic ubH2B is inversely correlated with burst size and PolI efficiency: genes were sorted according to the average ubH2B levels throughout the gene. Shown is the normalized noise (predicted burst size) and PolII efficiency, averaged over 400 genes sliding window. See also Figure S2 and Table S2.

enough to be detected by flow cytometry, yet not too high to ensure a significant contribution of noise intrinsic to the transcription process (Figure 1B). All promoters were inserted into the *HIS3* locus upstream of the reporter and were combined with the deletion mutants using Synthetic Genetic Array (SGA) (Tong and Boone, 2006). Altogether, we generated a set of 137X11 strains, each deleted of one chromatin regulator and carrying one YFP-driving promoter.

We used flow cytometry to measure the single-cell reporter expression in each strain. Promoters changed their expression in ~20%–30% of the deletions (Figure S1). The expression changes were moderate (~30%) and did not correlate with promoters' mean abundance or noise. This is consistent with a recent study showing that individual deletions of most chromatin regulators have minor effect on the transcription profile (Lenstra et al., 2011).

Burst-size is regulated by H2B ubiquitination and Set3-dependent deacetylation: From the distribution of expression levels, we calculated the predicted burst size and burst frequency. For this, we measured the coefficient of variation while gating for cell population of similar cell-cycle phase and size. Burst size was calculated by multiplying the coefficient of variation by the mean expression, while burst frequency was calculated as the inverse of the coefficient of variation, as noted above (Figure S2A). Significant effects of the deletions on burst size versus burst frequency were consistent between the different promoters.

We classified the genes into known complexes and functional groups (Table S1) and examined for consistent behavior (Figure 2A). Burst size was increased by deletions of *LGE1* and *RAD6*, genes required for H2B monoubiquitination at lysine residues 123 (ubH2B) (Robzyk et al., 2000). The predicted burst frequency was most strongly affected by histone acetylation: decreasing when acetyltrasferases were deleted (e.g., SAGA complex) and increasing in cells deleted of Rpd3(L)C components (*SAP30* and *PHO23*, although not *RPD3* itself) (Keogh et al., 2005). Surprisingly, the deletion of Set3C HDAC components (*SET3* and *HOS2*) increased the predicted burst size, but not burst frequency (Figures 1C, 1D, and 2A).

To further verify these results, we chose nine regulators, including components of the Set3C and Rpd3(L)C, as well as genes involved in ubiquitination, deubiquitination, methylation, and histone remodeling, and deleted them individually in ~200 additional reporter strains carrying different GFP-fused proteins (Table S2). Consistent with the results of the initial screen, burst frequency increased when deleting the *SAP30* component of Rpd3(L)C, while deletion of *SET3* or genes required for ubH2B (*RAD6*, *LGE1*), increased the predicted burst size. Further, preventing H2B ubiquitination via the *H2B-K123R* mutation (Robzyk et al., 2000) increased the predicted burst size of most

GFP-fused genes (Figures 2B and S2B). Taken together, this analysis suggests that ubH2B and Set3C-dependent deacetylation repress burst size in multiple genes.

ubH2B May Reduce Burst Size by Limiting PolII Processivity

Our analysis assigned ubH2B a role as a repressor of burst size. If the activity of ubH2B in reducing burst size is general, then highly ubiquitinated genes will be of low noise (per mean expression). To examine this prediction, we compared the genome-wide profile of ubH2B (Schulze et al., 2009) with the predicted burst size (normalized noise) of ~2,000 yeast GFP-fused proteins (Newman et al., 2006). Indeed, ubH2B levels were inversely correlated with the predicted burst size ($c = -0.37$, Figure 2C), supporting a general role of ubH2B in reducing burst size. We further noticed elevated levels of ubH2B at highly expressed genes ($c = 0.44$). Together, our results suggest that ubH2B is targeted to genes of high expression, where it acts to reduce burst size.

ubH2B can repress burst size by increasing the transition from permissive to nonpermissive chromatin state, thereby reducing burst duration. Such regulation would imply a role at gene promoter or 5′ gene end. ubH2B, however, is found primarily within the coding region and is relatively uniform there (Schulze et al., 2009) (Figure S2C). Furthermore, previous studies assigned ubH2B roles in transcription elongation: it stabilizes nucleosomes, promotes their reassembly (Chandrasekharan et al., 2009; Fleming et al., 2008), and is required for the elongation-promoting phosphorylation of PolII by Ctk1 (Wyce et al., 2007). Further, limiting H2B ubiquitination increases sensitivity to drugs interfering with transcriptional elongation (Kim and Buratowski, 2009; Wyce et al., 2007). Thus, ubH2B is more likely to affect burst size through its role in transcription elongation.

Burst size depends on PolII processivity, namely the probability that an elongating PolII will produce a functional transcript rather than terminating prematurely. PolII processivity is regulated at the level of transcription elongation and not transcription initiation (Mason and Struhl, 2005; Struhl, 2005; Zhang et al., 2007). We hypothesized that ubH2B reduces burst size by repressing PolII processivity. In support of that, preventing H2B ubiquitination by the *htb-K123R* mutation led to PolII processivity defects at the *GAL1* gene (Chandrasekharan et al., 2009; Fleming et al., 2008).

A measure that depends on PolII processivity, but is easier to measure, is PolII efficiency, which we define as the number of mRNA transcripts produced per gene-bound PolII (normalized to gene length). We therefore predicted that PolII efficiency will be low at genes that are of high ubH2B. To examine this, we defined PolII efficiency using the genome-wide binding data of the PolII Rpb3 subunit or the group of elongation factors (Mayer et al., 2010). mRNA levels were quantified using the data of Yassour et al., 2009 (Supplemental Experimental Procedures). As predicted, PolII efficiency correlates with burst size ($c = 0.25$; Figure S2F) and is inversely correlated with ubH2B ($c = -0.39$; Figures 2C and S2F). An independent measure for ubH2B levels is provided by the binding profile of Paf1, an elongation factor facilitating ubH2B (Kim and Roeder, 2009; Warner et al., 2007). Paf1 binding profile was strongly correlated with ubH2B level ($c = 0.69$) and was inversely correlated with PolII efficiency and burst size (Figure S2D).

PolII efficiency depends on PolII processivity, but may also be regulated by additional processes. For example, slowing elongation will decrease processivity (and burst size) only if increasing the probability of premature PolII termination, but will reduce efficiency even if not effecting processivity. As an additional, more direct measure of PolII processivity, we examined the decrease in PolII density along the gene, using the high-resolution data recently published (Churchman and Weissman, 2011). Indeed, consistent with ubH2B repressing PolII processivity, the decrease in PolII density along the gene was inversely correlated with ubH2B levels ($c = -0.28$) and also with Paf1 binding ($c = -0.39$) (Figures S2G and S2H).

Genome-wide Functions of Set3C and Rpd3(L)C

Our screen for noise regulators indicated that Set3C, like ubH2B effectors, reduces burst size. In contrast, Rpd3(L)C was predicted to reduce burst frequency, suggesting fundamentally different modes of action of these two HDACs. To more generally characterize the differences between Set3C and Rpd3(L)C, we applied ChIP-Seq to map H3K9 acetylation (H3K9ac) in five mutants, individually deleted for components of Set3C (*SET3* and *HOS2*) or Rpd3(L)C (*SAP30*, *PHO23*, and *RPD3*). Note that while the Sap30 and Pho23 are specific components of Rpd3(L)C, Rpd3 itself participates also in Rpd3(S) HDAC complex (Keogh et al., 2005). We profiled the H3K9ac mark since it correlates with gene expression (Liu et al., 2005; Robyr et al., 2002) and was previously used to analyze the activity of Set3C at individual genes (Kim and Buratowski, 2009; Liu et al., 2005).

Changes in acetylation were highly correlated between same-complex deletions (Figures 3A and S3A). For Rpd3(L)C, the two specific subunits (*SAP30* and *PHO23*) correlated significantly better than the nonspecific subunit *RPD3*, although all three were closer to each other than to the two Set3C components.

The data we obtained were of high enough resolution to define acetylation of single nucleosomes. H3K9ac is strongest at the +1 nucleosome, directly downstream of the transcription start site, and decreases gradually within the coding region (Figures 3B and S3C). A notable drop between the +1 and +2 nucleosomes suggests a +1 specific acetylation or +2 nucleosome specific deacetylation. All deletions increased acetylation primarily within the coding regions, as reflected by the sharper increase in acetylation between promoter and coding region in the mutants relative to wild-type (Figures 3B and S3C). This is in contrast with the common view that Rpd3(L)C acts preferentially in promoters, but is consistent with the recent work showing Rpd3(L)C binding also to coding regions (Drouin et al., 2010).

Gene Expression Correlates with H3 Acetylation Only at the 5′ End of Genes

Both Set3C and Rpd3(L)C were predicted to act as repressors of gene expression in our screen. Yet, we find them to preferentially deacetylate genes of high (Set3C) or medium (Rpd3(L)C) expression (Figures 3C, 3D, and S4A). Furthermore, while the role of Rpd3(L)C as a repressor is well established, previous studies have shown that Set3C is required for the rapid activation of the *GAL1* gene (Kim and Buratowski, 2009; Wang et al., 2002).

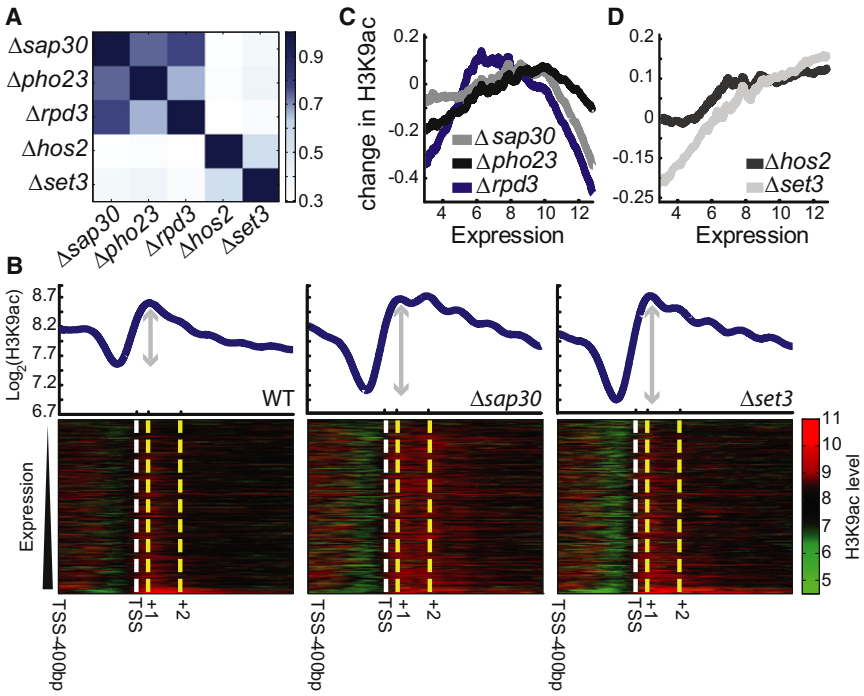

Figure 3. H3K9ac Profiles in Set3C and Rpd3(L)C HDAC Deletions

(A) Consistent profiles of Rpd3(L)C and Set3C components: correlation matrix (Pearson) between the log-ratio change in the acetylation profiles in the mutants relative to wild-type. Acetylation levels were averaged over the coding region, for up to 800 bp from the transcription start site (Xu et al., 2009).

(B) The pattern of H3K9ac: H3K9ac profile in wild-type and two mutants, as indicated. Genes were sorted by their wild-type expression (Yassour et al., 2009). The average acetylation along each gene is plotted at the top panel.

(C) Rpd3(L)C preferentially targets genes of mid expression: Genes were sorted by their wild-type expression. The (log2) change in gene acetylation is plotted for the indicated mutants, averaged over a sliding window of 400 genes. The decrease in Rpd3(L)C effect at highly expressed genes remains also when ribosomal proteins are excluded (Figure S4A).

(D) Set3C preferentially targets genes of high expression: same as (C) for deletion of Set3C components. See also Figure S3.

To verify their role as repressors of gene expression, we examined the relationship between H3K9ac, HDAC activity, and gene expression.

The total H3K9ac over a gene increases with gene expression (c = 0.4), consistent with previous reports (Liu et al., 2005; Pokholok et al., 2005). Our high-resolution data demonstrate, however, that this correlation varies along gene positions, with high correlation at the 5′ end but considerably lower correlations at downstream nucleosomes (Figure 4A). In fact, gene expression does not correlate with H3K9ac downstream of the +4 nucleosome. Thus, H3K9ac peaks at the +1 nucleosome where it is highly correlated with gene expression and gradually decreases at subsequent nucleosomes while losing the correlation with gene expression.

We next used published gene expression profiles in these mutants (Lenstra et al., 2011) and compared the expression changes with the changes in H3K9ac. In all mutants, changes in expression and acetylation were correlated. The correlations are rather small, in particular for the Set3C deletions that had a moderate effect on gene expression (Figure 4B). In all mutants, changes of +2 nucleosome acetylation best predicted expression changes. Together, these results support the notion that both Rpd3(L)C and, to a lesser extent, Set3C, act as repressors of gene expression.

Evidence that Set3C Reduces Burst Size by Repressing PolII Processivity

We predicted that genes targeted by Set3C are of low normalized noise, reflecting Set3C's role in reducing burst size. Indeed, comparing our acetylation profiles with the available large-scale noise measurements (Newman et al., 2006), we find that Set3C preferentially targets genes of low predicted burst size. In contrast, Rpd3(L)C preferentially targets genes of high predicted burst size (Figures 5C, 5D, and S4B).

We hypothesize that, similarly to ubH2B, Set3C represses burst size of highly expressed genes by reducing PolII processivity. Consistent with a role in elongation, Set3C acts preferentially within the coding region and affects nucleosomes relatively uniformly (Figure 5A). In contrast, Rpd3(L)C acts preferentially at the 5′ end of genes, and specifically at the +2 nucleosomes. In fact, the decrease in H3K9ac between the +1 and +2 nucleosomes is completely lost in all three strains deleted of Rpd3(L)C components (Figures 5B and S3B). The activity of Rpd3(L)C at the +2 nucleosome suggests a postrecruitment step in transcription initiation. Notably, it was shown that genes of medium expression accumulate PolII at the 5′ gene end, consistent with these genes being the preferred targets of Rpd3(L)C (Venters and Pugh, 2009; Wade and Struhl, 2008).

Furthermore, we find that Set3C preferentially targets genes of low PolII efficiency. In contrast, Rpd3(L)C targets are of mid to high PolII efficiency (Figures 5E, 5F, S4C, and S4D). As explained above, PolII efficiency is a surrogate for PolII processivity, supporting the idea that Set3C reduces burst size by increasing the chance that the polymerase will abort transcription. Consistent with that, the spatial decay of PolII throughout genes was faster in Set3C targets (Figure S2H).

ubH2B Promotes Set3-Dependent H3K9ac

Previous studies linked Set3C recruitment to ubH2B. First, at least in some cases, Set3C was recruited by H3K4 dimethylation, a modification that requires Set1 recruitment by ubH2B (Kim and Buratowski, 2009). Second, ubH2B may also promote Set3C function through Paf1, in a Set1-indepenent manner (Lenstra et al., 2011). We therefore hypothesized that ubH2B

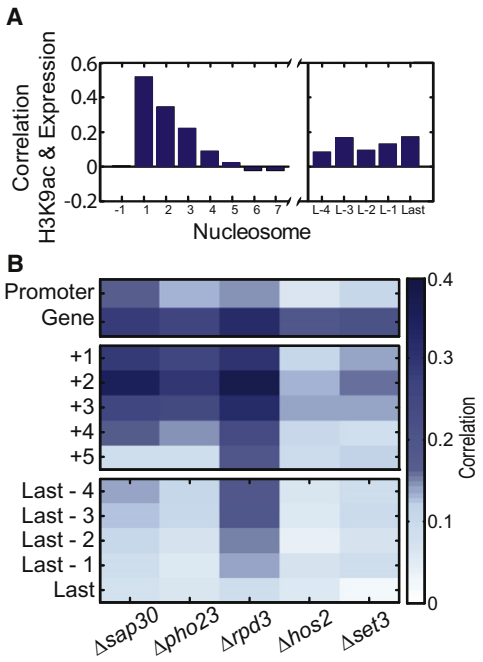

Figure 4. Correlations between Gene Expression, H3K9ac, and HDAC Activity

(A) Gene expression correlates with H3K9ac only at the 5′ gene end: Pearson correlations between wild-type expression and H3K9ac levels at each nucleosome. Note that H3K9ac signal strength at +5, +6, and +7 is the same as at the 3′ gene end where H3K9ac and gene expression are correlated.

(B) Changes in expression are correlated with changes in H3K9ac: gene expression data were taken from published data set (Lenstra et al., 2011) and were correlated with the change in H3K9ac. Promoter acetylation is approximated by the H3K9ac levels at the −1 nucleosome. Changes in acetylation were averaged over all genes at the relevant regions.

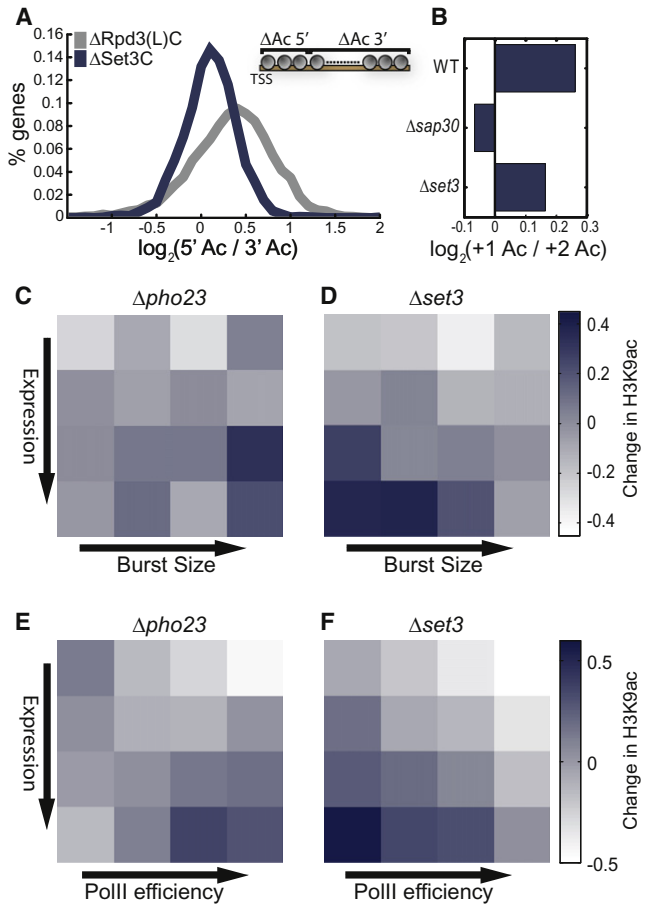

Figure 5. Gene Targets of Rpd3(L)C and Set3C

(A) Activities of Set3C and Rpd3(L)C along the coding region: for each mutant, the ratio between the (log2) change in H3K9ac at gene beginning (TSS through TSS + 400 bp) and at gene end (TSS + 400 through gene end) was measured. Shown is the histogram of this ratio, averaged for two mutants of each complex (*Δsap30*, *Δpho23* for Rpd3(L)C and *Δhos2*, *Δset3* for Set3C).

(B) The decrease in H3K9ac at the +2 versus +1 nucleosomes depends on Rpd3(L)C: the (log2) ratio between H3K9ac levels at the +1 versus the +2 nucleosomes in the indicated mutants.

(C–F) Burst size and PolII efficiency of target genes: genes were ordered into 16 groups based on gene expression and burst size (or PolII efficiency, as indicated). Shown is the average change in H3K9ac for each group and indicated mutant. For burst size, the analysis was restricted to the ~2,000 genes where data is available, while PolII efficiency was defined for all genes. In each mutant, changes in H3K9ac were normalized to a mean of 0 and standard deviation of 1 to allow easier comparisons. See also Figure S4.

and Set3C repress burst size through the same pathway and asked whether our data support such a link.

As a first indication that ubH2B promotes Set3C function, we observed that Set3C (but not Rpd3(L)C) preferentially deacetylates genes of high ubH2B and high Paf1 occupancy (Figure 6D). We further expected an inverse correlation between acetylation and ubH2B, but reasoned that such correlation may be hindered by the mutual dependence of both H3K9ac and ubH2B on gene expression (Henikoff and Shilatifard, 2011; Kim and Buratowski, 2009; Lickwar et al., 2009). Following our observations that expression correlates with H3K9ac at gene beginning only, we examined the correlation between H3K9ac and ubH2B at individual nucleosomes, expecting to observe an inverse correlation between ubH2B and H3K9ac at downstream nucleosomes.

As predicted, we find that gene ubH2B levels correlate with H3K9ac at the +1 nucleosome, but this correlation vanishes rapidly at downstream nucleosomes (Figures 6B and S5A). In fact, an inverse correlation between the gene average ubH2B and H3K9ac was apparent for all positions downstream of +3 nucleosomes. Thus, in most regions inside genes, higher average ubH2B is associated with lower acetylation, suggesting that ubH2B promotes deacetylation, as predicted.

To further support the idea that the spatially varying correlation pattern we observe reflects the mutual dependence of ubH2B and H3K9ac on gene transcription, we grouped genes based on expression levels and analyzed the correlation between ubH2B and H3K9ac within each group (Figures 6A and 6B). We found negative correlation between ubH2B and average gene H3K9ac in genes of mid expression, while highly expressed genes showed no correlation and lowly expressed genes showed positive correlation. To further understand the difference between the expression levels, we looked at the

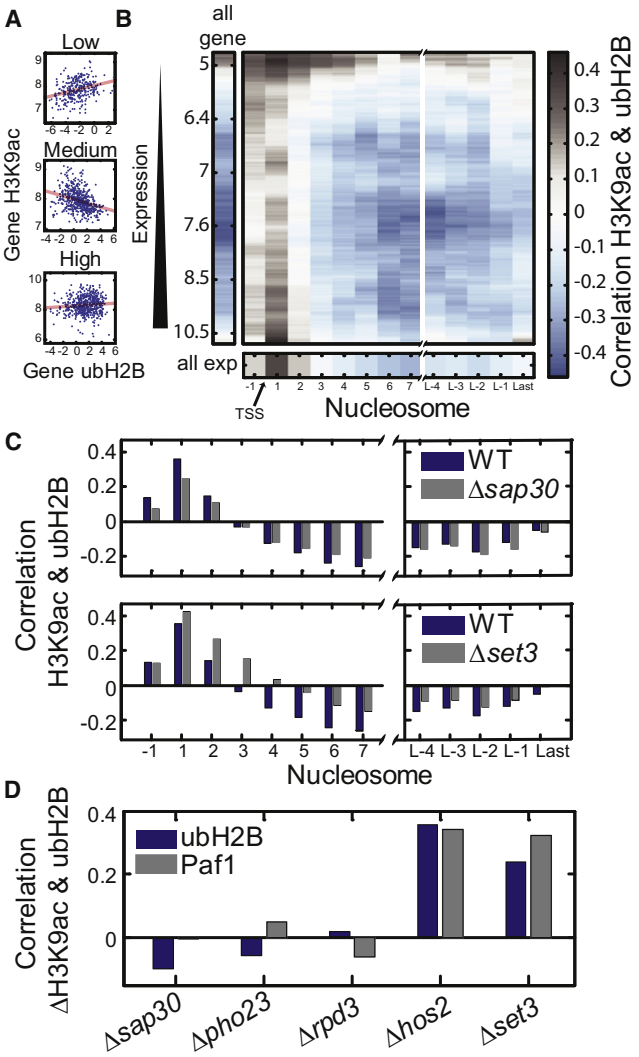

Figure 6. Correlation between ubH2B and H3K9ac

(A and B) The correlation between H3K9ac and ubH2B depends on gene expression and nucleosome position. Shown in (A): H3K9ac profile as a function of gene ubH2B for the 10% lowest-expressed genes, 10% of medium-expressed genes, and 10% highest-expressed genes, as indicated. Linear fit is shown in red. The center plot in (B) shows the correlation between H3K9ac at particular nucleosome and the gene average ubH2B for gene groups of different expression. Each correlation value was measured for a window of 500 genes, centered at the indicated expression. The correlation of ubH2B with gene average H3K9ac is shown at the left, whereas the correlation between ubH2B and the nucleosome-specific H3K9ac for all expression level is shown on the bottom (see also Figure S5A for a similar plot describing correlation between H3K9ac and PAF1 binding).

(C) Deletion of Set3C eliminates the negative correlation between H3K9ac and ubH2B: correlation between gene average ubH2B and H3K9ac at different nucleosomes is plotted for WT (same as in B, bottom), as well as strains deleted of *SAP30* or *SET3*.

(D) Set3C preferentially targets genes of high ubH2B.The average Rank correlation between gene average ubH2B (or Paf1 binding) and changes in gene H3K9ac is shown for the different mutants. See also Figure S5.

correlations at individual nucleosomes. While high-expressed genes showed negative correlation downstream inside the gene, low-expressed genes didn't. We hypothesized that the two phenomena are due to the coupling of both modifications to transcription process. While in the low-expressed genes histone ubiquitination is mostly not present, in high-expressed genes the high level of histone acetylase activity dominates the H3K9ac pattern over the effect of deacetylation.

Together, our analysis supports the idea that ubH2B promotes deacetylation. To examine whether ubH2B functions through Set3C, we examined the correlation between ubH2B and H3K9ac in the different deletion mutants. Deletion of Rpd3(L)C-specific subunits (*Δsap30* or *Δpho23*) had no effect on the correlation pattern, while deletion of the Set3C subunits reduced the negative correlation between ubH2B and H3K9ac in all nucleosomes and at all expression levels (Figures 6C and S5B–S5D). Notably, even in Set3C mutants, a negative correlation was still observed in nucleosomes closer to the 3′ gene end, suggesting that ubH2B recruits additional HDACs.

H3K9ac Profiles of Mutants Deleted of ubH2B Effectors Support Set3C Recruitment by ubH2B

Our analysis supports a genome-wide link between ubH2B and Set3C. To more directly examine the prediction that ubH2B promotes Set3C-dependent deacetylation, we mapped the H3K9ac profile in mutants deleted of two H2B ubiquitinating enzymes (*Δbre1* and *Δrad6*) and two H2B deubquitinating enzymes (*Δubp8* and *Δubp10*). Due to technical reasons, the resolution of these ChIP-Seq data was lower than that of the deacetylation mutants analyzed above, and we therefore consider only the gene-averaged profile (rather than single nucleosomes).

As predicted, deletion of *BRE1* or *RAD6* increased acetylation preferentially at Set3-dependent genes and genes of high ubH2B (Figures 7A, 7B, and S6B–S6F). Further, consistent with a function of ubH2B in reducing PolII efficiency, both mutants affected preferentially genes of low PolII efficiency (Figures 7C and S6G–S6I). Those results directly support the recruitment of Set3C by ubH2B to genes of high expression and low noise.

Notably, the H3K9ac profiles in the strains deleted of *UBP8* or *UBP10* did not correlate with the profiles of Set3C deletions (Figures 7B and S6D). This is consistent with the limited impact of *UBP8* on burst size, predicted by our screen, and also with a recent report showing that deleting *UBP8* or *UBP10* does not change the profiles of PolII binding or histone methylation (Schulze et al., 2011).

DISCUSSION

Our study began with the theoretical observation that gene expression variance (noise) can distinguish mechanisms of gene expression regulation (Friedman et al., 2006; Raj et al., 2006; Tan and van Oudenaarden, 2010). Applying this approach to 137 chromatin-associated factors suggested distinct roles of the Set3C and Rpd3(L)C HDACs. In our assay, both complexes repressed the expression of multiple reporter genes, yet appeared to function through distinct mechanisms: Rpd3(L)C

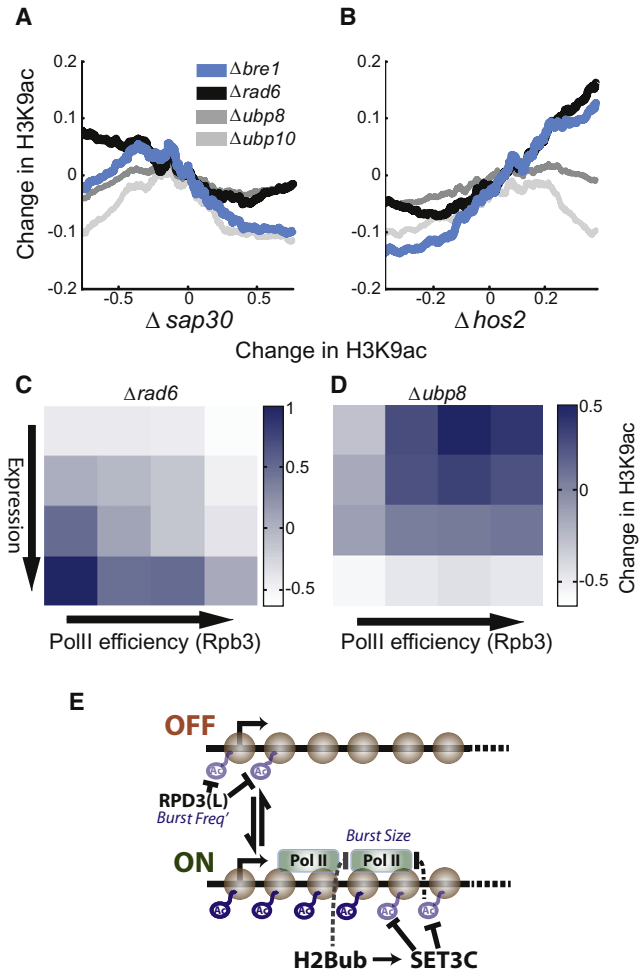

Figure 7. H3K9ac Profiles in Mutants Deleted of Ubiquitination and Deubiquitination Enzymes

(A and B) Deletion of *BRE1* or *RAD6* increases acetylation of Set3C-dependent genes. Genes were sorted by average change in H3K9ac in strains deleted of *SAP30* (A) or *HOS2* (B). The (log2) change in acetylation in the indicated mutants is shown. H3K9ac values were averaged over 400 genes sliding window.

(C and D) Bre1 targets genes of high expression and low PolII efficiency. Genes were ordered into 16 groups based on gene expression and PolII efficiency. Shown is the average change in H3K9ac at the indicated mutant for each group. In each mutant, changes in H3K9ac were normalized to a mean of 0 and standard deviation of 1, to allow an easier comparison (see also Figures S6G–S6J for other mutants).

(E) Graphic model summarizing the results. In the prevailing model of gene expression, genes are made in bursts, namely period of extensive expression interspaced by time intervals in which expression is negligible. This is captured by assuming that gene can be at two states: a state permissive for expression (ON) and a state that is not permissive (OFF). The rate of transition from the OFF to ON state defines the burst frequency, while the number of proteins made per burst event defines the burst size. Gene expression can be regulated through changes in either burst frequency or burst size. Our results indicated that Rpd3(L)C represses burst frequency, probably by deacetylation of nucleosomes at the beginning of a gene (+2 in particular). In contrast, Set3C and ubH2B are predicted to repress burst size by reducing PolII processivity. ubH2B and Set3C likely function within the same pathway, to modulate nucleosomes within the gene. See also Figure S6.

modulated the predicted burst frequency while Set3C modulated the predicted burst size, as did ubH2B. Using genome-wide profiling of H3K9ac, we further characterized the HDAC activities of Set3C and Rpd3(L)C.

Previous studies associated both ubH2B and Set3C with transcription elongation (Fleming et al., 2008; Kim and Buratowski, 2009). This is also evident from the high correlation between expression level and ubH2B inside the gene. We suggest that this reflects the coupling of ubH2B to the transcription machinery, rather than a role for ubH2B in promoting transcription. Consistent with that, we find that Set3C functions relatively uniformly in coding region. Based on our data, we further refined the role of ubH2B and Set3C in elongation, suggesting that they act to decrease PolII processivity, namely the probability that an elongating PolII will produce a functional transcript. Other elongation factors may not influence burst size or could even have an opposite effect. For example, TFIIS (*DST1* in yeast) increases PolII processivity (Mason and Struhl, 2005). Notably, recent work in humans has shown that ubH2B inhibits the ability of TFIIS to relieve stalled PolII (Shema et al., 2011). Thus, both the increase of PolII processivity by TFIIS and its inhibition by ubH2B appear to be conserved between yeast and human.

How could ubH2B and Set3C reduce PolII processivity? Both ubH2B and deacetylation can stabilize nucleosomes (Chandrasekharan et al., 2009; Henikoff and Shilatifard, 2011; Kurdistani and Grunstein, 2003). Higher nucleosome stability may interfere with PolII progression and increase the probability of pausing or premature termination. Alternatively, factors that actively promote premature PolII termination might be recruited in an ubH2B- or Set3C-dependent manner. There are examples for such active recruitment of the Nrd1-Nab3-Sen1 termination complex (Kim and Levin, 2011; Terzi et al., 2011). Thus, the Paf1 complex, which is required for ubH2B, also recruits Sen1 to repress the *FKS2* gene. ubH2B and H3K4 dimethylation were also associated with this recruitment (Kim and Levin, 2011). This pathway, however, functions mostly in the regulation of snoRNA and acts at the 5′ end of genes (Sheldon et al., 2005; Steinmetz et al., 2006). In contrast, most of the effects we observe occur within coding regions.

Our data support a general role of ubH2B in promoting Set3C-dependent deacetylation, suggesting that they function through the same pathway. ubH2B may promote Set3C function indirectly, by recruiting Set1 and thereby promoting H3K4 dimethylation. Alternatively, ubH2B promotes Set3C function primarily through a process independent of Set1, as was suggested recently (Lenstra et al., 2011). We favor this latter hypothesis since Set3C did not appear to prefer genes of high H3K4 di- or trimethylation (Pokholok et al., 2005) (Figure S6A). Further, in our screen, deletion of *SET1* did not increase burst size, although this result is hard to interpret due to the severe growth limitation of this strain. Notably, the effect of ubH2B on burst size is consistently stronger than that of Set3C, suggesting that ubH2B effects burst size both by facilitating Set3C function and by additional means.

More generally, the high resolution of our data enabled characterizing acetylation at the level of single nucleosomes. We found that transcription-dependent acetylation is localized to

the 5′ end of genes, but is largely absent from mid-gene and downstream. Analysis of these nucleosomes can therefore be used to identify direct interactions between different chromatin marks, as we demonstrated in the context of ubH2B-dependent recruitment of Set3C. We anticipated that, as sequencing technologies become more efficient, similar high-resolution spatial analysis can be used to distinguish direct from indirect effects of chromatin modifications.

Our study suggests that gene expression noise depends on specific regulatory factors that function at only a subset of genes. Noise may therefore be subject to selection independent of mean expression. Tuning noise levels may be beneficial: some genes are required at precise amount, while noise in others could provide diversity to an otherwise genetically identical population. It will be interesting to examine whether noise levels diversified during evolution and whether this diversity was driven, at least in part, by changing the function or specificity of chromatin factors such as the ubiquitination or deacetylation enzymes.

EXPERIMENTAL PROCEDURES

Strains and Media

Construction of strains for noise screen was done by SGA method (Tong et al., 2001) with minor extensions. GFP-fusion strains were taken from the yeast GFP clone collection. The ChIP-Seq experiments were done on BY4741 strains. Full list of strains can be found in Tables S1 and S2.

Flow Cytometry

GFP fluorescence was measured for stains in logarithmic growth stage using LSRII flow cytometer fitted with HTS sampler (Becton Dickinson). Analysis and gating of FACS measurements are described in Supplemental Experimental Procedures.

ChIP-Seq

Chromatin immunoprecipitation was done as described previously (Liu et al., 2005), with some modifications. Samples were sonicated with bioruptor sonicator for 60 min (30 s intervals) and precipitated with H3K9-acetyl antibody (Abcam ab12179) and conjugated to protein A beads.

High-throughput sequencing was done using Illumina GAII system for most samples and HiSeq2000 for Δ*bre1*, Δ*rad6*, Δ*ubp8*, Δ*ubp10*, and a second WT. Analysis of the high-throughput sequencing, definition of PolII efficiency, and definition of nucleosome and gene regions are described in Supplemental Experimental Procedures.

ACCESSION NUMBERS

ChIP-Seq data files described in this study are published in the SRA database under accession number SRA051855.1.

SUPPLEMENTAL INFORMATION

Supplemental Information includes six figures, two tables, and Supplemental Experimental Procedures and can be found with this article online at doi:10.1016/j.molcel.2012.05.008.

ACKNOWLEDGMENTS

We thank Sagi Levy and Ilya Soifer for remarks on the manuscript, Yaron Mosseson and Dalia Rosin-Grunewald for experimental help, Dima Lukatsky for starting the project, Shirley Horn-Saban, and members of our group for discussions. This work was supported by NIH (P50GM068763), the ERC, The Israel Science Foundation, and the Hellen and Martin Kimmel award for innovative investigations.

Received: September 4, 2011
Revised: March 7, 2012
Accepted: May 4, 2012
Published online: June 7, 2012

REFERENCES

Bar-Even, A., Paulsson, J., Maheshri, N., Carmi, M., O'Shea, E., Pilpel, Y., and Barkai, N. (2006). Noise in protein expression scales with natural protein abundance. Nat. Genet. *38*, 636–643.

Barkai, N., and Shilo, B.Z. (2007). Variability and robustness in biomolecular systems. Mol. Cell *28*, 755–760.

Blake, W.J., KAErn, M., Cantor, C.R., and Collins, J.J. (2003). Noise in eukaryotic gene expression. Nature *422*, 633–637.

Blake, W.J., Balázsi, G., Kohanski, M.A., Isaacs, F.J., Murphy, K.F., Kuang, Y., Cantor, C.R., Walt, D.R., and Collins, J.J. (2006). Phenotypic consequences of promoter-mediated transcriptional noise. Mol. Cell *24*, 853–865.

Cai, L., Friedman, N., and Xie, X.S. (2006). Stochastic protein expression in individual cells at the single molecule level. Nature *440*, 358–362.

Cairns, B.R. (2009). The logic of chromatin architecture and remodelling at promoters. Nature *461*, 193–198.

Chandrasekharan, M.B., Huang, F., and Sun, Z.W. (2009). Ubiquitination of histone H2B regulates chromatin dynamics by enhancing nucleosome stability. Proc. Natl. Acad. Sci. USA *106*, 16686–16691.

Churchman, L.S., and Weissman, J.S. (2011). Nascent transcript sequencing visualizes transcription at nucleotide resolution. Nature *469*, 368–373.

Drouin, S., Laramée, L., Jacques, P.E., Forest, A., Bergeron, M., and Robert, F. (2010). DSIF and RNA polymerase II CTD phosphorylation coordinate the recruitment of Rpd3S to actively transcribed genes. PLoS Genet. *6*, e1001173.

Elowitz, M.B., Levine, A.J., Siggia, E.D., and Swain, P.S. (2002). Stochastic gene expression in a single cell. Science *297*, 1183–1186.

Field, Y., Fondufe-Mittendorf, Y., Moore, I.K., Mieczkowski, P., Kaplan, N., Lubling, Y., Lieb, J.D., Widom, J., and Segal, E. (2009). Gene expression divergence in yeast is coupled to evolution of DNA-encoded nucleosome organization. Nat. Genet. *41*, 438–445.

Fleming, A.B., Kao, C.F., Hillyer, C., Pikaart, M., and Osley, M.A. (2008). H2B ubiquitylation plays a role in nucleosome dynamics during transcription elongation. Mol. Cell *31*, 57–66.

Friedman, N., Cai, L., and Xie, X.S. (2006). Linking stochastic dynamics to population distribution: an analytical framework of gene expression. Phys. Rev. Lett. *97*, 168302.

Henikoff, S., and Shilatifard, A. (2011). Histone modification: cause or cog? Trends Genet..

Keogh, M.C., Kurdistani, S.K., Morris, S.A., Ahn, S.H., Podolny, V., Collins, S.R., Schuldiner, M., Chin, K., Punna, T., Thompson, N.J., et al. (2005). Cotranscriptional set2 methylation of histone H3 lysine 36 recruits a repressive Rpd3 complex. Cell *123*, 593–605.

Kim, T., and Buratowski, S. (2009). Dimethylation of H3K4 by Set1 recruits the Set3 histone deacetylase complex to 5′ transcribed regions. Cell *137*, 259–272.

Kim, K.Y., and Levin, D.E. (2011). Mpk1 MAPK association with the Paf1 complex blocks Sen1-mediated premature transcription termination. Cell *144*, 745–756.

Kim, J., and Roeder, R.G. (2009). Direct Bre1-Paf1 complex interactions and RING finger-independent Bre1-Rad6 interactions mediate histone H2B ubiquitylation in yeast. J. Biol. Chem. *284*, 20582–20592.

Kurdistani, S.K., and Grunstein, M. (2003). Histone acetylation and deacetylation in yeast. Nat. Rev. Mol. Cell Biol. *4*, 276–284.

Lenstra, T.L., Benschop, J.J., Kim, T., Schulze, J.M., Brabers, N.A., Margaritis, T., van de Pasch, L.A., van Heesch, S.A., Brok, M.O., Groot Koerkamp, M.J., et al. (2011). The specificity and topology of chromatin interaction pathways in yeast. Mol. Cell *42*, 536–549.

Lickwar, C.R., Rao, B., Shabalin, A.A., Nobel, A.B., Strahl, B.D., and Lieb, J.D. (2009). The Set2/Rpd3S pathway suppresses cryptic transcription without regard to gene length or transcription frequency. PLoS ONE *4*, e4886.

Liu, C.L., Kaplan, T., Kim, M., Buratowski, S., Schreiber, S.L., Friedman, N., and Rando, O.J. (2005). Single-nucleosome mapping of histone modifications in S. cerevisiae. PLoS Biol. *3*, e328.

Mason, P.B., and Struhl, K. (2005). Distinction and relationship between elongation rate and processivity of RNA polymerase II in vivo. Mol. Cell *17*, 831–840.

Mayer, A., Lidschreiber, M., Siebert, M., Leike, K., Söding, J., and Cramer, P. (2010). Uniform transitions of the general RNA polymerase II transcription complex. Nat. Struct. Mol. Biol. *17*, 1272–1278.

Newman, J.R., Ghaemmaghami, S., Ihmels, J., Breslow, D.K., Noble, M., DeRisi, J.L., and Weissman, J.S. (2006). Single-cell proteomic analysis of S. cerevisiae reveals the architecture of biological noise. Nature *441*, 840–846.

Ozbudak, E.M., Thattai, M., Kurtser, I., Grossman, A.D., and van Oudenaarden, A. (2002). Regulation of noise in the expression of a single gene. Nat. Genet. *31*, 69–73.

Paulsson, J. (2004). Summing up the noise in gene networks. Nature *427*, 415–418.

Pavri, R., Zhu, B., Li, G., Trojer, P., Mandal, S., Shilatifard, A., and Reinberg, D. (2006). Histone H2B monoubiquitination functions cooperatively with FACT to regulate elongation by RNA polymerase II. Cell *125*, 703–717.

Pokholok, D.K., Harbison, C.T., Levine, S., Cole, M., Hannett, N.M., Lee, T.I., Bell, G.W., Walker, K., Rolfe, P.A., Herbolsheimer, E., et al. (2005). Genome-wide map of nucleosome acetylation and methylation in yeast. Cell *122*, 517–527.

Raj, A., Peskin, C.S., Tranchina, D., Vargas, D.Y., and Tyagi, S. (2006). Stochastic mRNA synthesis in mammalian cells. PLoS Biol. *4*, e309.

Raser, J.M., and O'Shea, E.K. (2004). Control of stochasticity in eukaryotic gene expression. Science *304*, 1811–1814.

Raser, J.M., and O'Shea, E.K. (2005). Noise in gene expression: origins, consequences, and control. Science *309*, 2010–2013.

Rinott, R., Jaimovich, A., and Friedman, N. (2011). Exploring transcription regulation through cell-to-cell variability. Proc. Natl. Acad. Sci. USA *108*, 6329–6334.

Robyr, D., Suka, Y., Xenarios, I., Kurdistani, S.K., Wang, A., Suka, N., and Grunstein, M. (2002). Microarray deacetylation maps determine genome-wide functions for yeast histone deacetylases. Cell *109*, 437–446.

Robzyk, K., Recht, J., and Osley, M.A. (2000). Rad6-dependent ubiquitination of histone H2B in yeast. Science *287*, 501–504.

Schulze, J.M., Jackson, J., Nakanishi, S., Gardner, J.M., Hentrich, T., Haug, J., Johnston, M., Jaspersen, S.L., Kobor, M.S., and Shilatifard, A. (2009). Linking cell cycle to histone modifications: SBF and H2B monoubiquitination machinery and cell-cycle regulation of H3K79 dimethylation. Mol. Cell *35*, 626–641.

Schulze, J.M., Hentrich, T., Nakanishi, S., Gupta, A., Emberly, E., Shilatifard, A., and Kobor, M.S. (2011). Splitting the task: Ubp8 and Ubp10 deubiquitinate different cellular pools of H2BK123. Genes Dev. *25*, 2242–2247.

Sheldon, K.E., Mauger, D.M., and Arndt, K.M. (2005). A Requirement for the Saccharomyces cerevisiae Paf1 complex in snoRNA 3′ end formation. Mol. Cell *20*, 225–236.

Shema, E., Kim, J., Roeder, R.G., and Oren, M. (2011). RNF20 inhibits TFIIS-facilitated transcriptional elongation to suppress pro-oncogenic gene expression. Mol. Cell *42*, 477–488.

Shilatifard, A. (2006). Chromatin modifications by methylation and ubiquitination: implications in the regulation of gene expression. Annu. Rev. Biochem. *75*, 243–269.

Steinmetz, E.J., Ng, S.B., Cloute, J.P., and Brow, D.A. (2006). cis- and trans-Acting determinants of transcription termination by yeast RNA polymerase II. Mol. Cell. Biol. *26*, 2688–2696.

Struhl, K. (2005). Transcriptional activation: mediator can act after preinitiation complex formation. Mol. Cell *17*, 752–754.

Tan, R.Z., and van Oudenaarden, A. (2010). Transcript counting in single cells reveals dynamics of rDNA transcription. Mol. Syst. Biol. *6*, 358.

Terzi, N., Churchman, L.S., Vasiljeva, L., Weissman, J., and Buratowski, S. (2011). H3K4 trimethylation by Set1 promotes efficient termination by the Nrd1-Nab3-Sen1 pathway. Mol. Cell. Biol. *31*, 3569–3583.

Tirosh, I., and Barkai, N. (2008). Two strategies for gene regulation by promoter nucleosomes. Genome Res. *18*, 1084–1091.

Tong, A.H., and Boone, C. (2006). Synthetic genetic array analysis in Saccharomyces cerevisiae. Methods Mol. Biol. *313*, 171–192.

Tong, A.H., Evangelista, M., Parsons, A.B., Xu, H., Bader, G.D., Pagé, N., Robinson, M., Raghibizadeh, S., Hogue, C.W., Bussey, H., et al. (2001). Systematic genetic analysis with ordered arrays of yeast deletion mutants. Science *294*, 2364–2368.

Venters, B.J., and Pugh, B.F. (2009). A canonical promoter organization of the transcription machinery and its regulators in the Saccharomyces genome. Genome Res. *19*, 360–371.

Wade, J.T., and Struhl, K. (2008). The transition from transcriptional initiation to elongation. Curr. Opin. Genet. Dev. *18*, 130–136.

Wang, A., Kurdistani, S.K., and Grunstein, M. (2002). Requirement of Hos2 histone deacetylase for gene activity in yeast. Science *298*, 1412–1414.

Warner, M.H., Roinick, K.L., and Arndt, K.M. (2007). Rtf1 is a multifunctional component of the Paf1 complex that regulates gene expression by directing cotranscriptional histone modification. Mol. Cell. Biol. *27*, 6103–6115.

Wyce, A., Xiao, T., Whelan, K.A., Kosman, C., Walter, W., Eick, D., Hughes, T.R., Krogan, N.J., Strahl, B.D., and Berger, S.L. (2007). H2B ubiquitylation acts as a barrier to Ctk1 nucleosomal recruitment prior to removal by Ubp8 within a SAGA-related complex. Mol. Cell *27*, 275–288.

Xu, Z., Wei, W., Gagneur, J., Perocchi, F., Clauder-Münster, S., Camblong, J., Guffanti, E., Stutz, F., Huber, W., and Steinmetz, L.M. (2009). Bidirectional promoters generate pervasive transcription in yeast. Nature *457*, 1033–1037.

Yassour, M., Kaplan, T., Fraser, H.B., Levin, J.Z., Pfiffner, J., Adiconis, X., Schroth, G., Luo, S., Khrebtukova, I., Gnirke, A., et al. (2009). Ab initio construction of a eukaryotic transcriptome by massively parallel mRNA sequencing. Proc. Natl. Acad. Sci. USA *106*, 3264–3269.

Zenklusen, D., Larson, D.R., and Singer, R.H. (2008). Single-RNA counting reveals alternative modes of gene expression in yeast. Nat. Struct. Mol. Biol. *15*, 1263–1271.

Zhang, Z., Klatt, A., Henderson, A.J., and Gilmour, D.S. (2007). Transcription termination factor Pcf11 limits the processivity of Pol II on an HIV provirus to repress gene expression. Genes Dev. *21*, 1609–1614.